Self-Assembly of Poly(oxybutylene)−Poly(oxyethylene)−Poly(oxybutylene) ($B_6E_{46}B_6$) Triblock Copolymer in Aqueous Solution

Tianbo Liu,[†] Zukang Zhou,[†,||] Chunhung Wu,[†,▽] Benjamin Chu,*[,†,‡] Dieter K. Schneider,[§] and Vaughn M. Nace[⊥]

Department of Chemistry, State University of New York at Stony Brook, Stony Brook, New York 11794-3400, Department of Material Sciences and Engineering, State University of New York at Stony Brook, Stony Brook, New York 11794-2275, Biology Department, Brookhaven National Laboratory, Upton, New York 11973, and The Dow Chemical Company, Freeport, Texas 77541

Received: November 15, 1996; In Final Form: January 14, 1997[⊗]

Laser light scattering and small-angle neutron scattering were used to study poly(oxybutylene)−poly(oxyethylene)−poly(oxybutylene) triblock copolymers ($B_6E_{46}B_6$) in aqueous solution from low to high concentrations and over a range of temperatures from 5 to 35 °C. $B_6E_{46}B_6$ molecules exist as unimers at low concentrations and low temperatures. At higher concentrations and at low temperature (≤15 °C), they associate in small numbers and scattering evidence shows that molecular associates with open structures might form. At higher temperatures, typical flowerlike micelles form. The critical micelle concentration decreases with increasing temperature while the association number increases. At high polymer concentrations (e.g., at 35% in mass), further entanglements form among the micelles, yielding another slow mode in dynamic light scattering, which can be attributed to the bridging of two hydrophobic end blocks located in two different hydrophobic clusters by the hydrophilic middle block. However, these cross-linkings were quite weak and free micelles were still the majority in solution. When the temperature is lowered, a very slow process of microphase separation occurs. The self-assembly behavior of $B_6E_{46}B_6$ is compared with that of other BEB type triblock copolymers.

Introduction

Block copolymers have attracted a great deal of attention because of their importance in many industrial applications. Extensive fundamental studies, mainly concerned with the micelle formation and the structural characteristics of polymeric micelles of diblock and triblock copolymers, have been reported.[1] Recently, a general theory for microstuctures in block copolymers with strongly interacting groups has also been proposed.[2] A solvent is considered selective if it is a thermodynamically good solvent for one block but a comparatively poor solvent for the other block. For ABA type triblock copolymers, the use of a selective solvent for the middle block can lead to a variety of possible self-assembled structures. First, flowerlike micelles are formed in which the central block takes on a loop conformation and its two end blocks become a part of the micellar core. Second, the assembly into a branched structure at low concentrations or a gellike network at high concentrations may occur because of the possible bridging function from the extended soluble middle block between the small clusters formed by the poorly solvated end blocks. The intermediate situation will be that some of the coronal middle blocks show a looping geometry, while some other middle blocks may have one of the end blocks dangling in solution.

Due to this uncertainty, the nature of the supramolecular structures of triblock copolymers in a selective solvent for the middle block becomes more difficult to predict, and therefore, has become a topic of interest. Different theoretical estimates on the entropy loss due to the loop formation were also derived, leading to conflicting conclusions about the reality of micelle formation.[3,4] Raspaud et al.[5] reported that for the polystyrene−polyisoprene−polystyrene triblock copolymers in tetrahydrofuran, a selective solvent for the middle block, loose open-associated aggregates could be formed. For $B_mE_nB_m$ and $P_mE_nP_m$ (poly(oxypropylene)−poly(oxyethylene)−poly(oxypropylene)) type triblock copolymers, several papers concerning their self-assembly behavior in aqueous solution have been presented by Yang et al. ($B_4E_{40}B_4$, $B_5E_{39}B_5$, and $B_7E_{40}B_7$)[6,7] and Zhou et al. ($P_{14}E_{24}P_{14}$, $B_5E_{91}B_5$, and $B_{12}E_{260}B_{12}$).[8−10] Generally, flowerlike micelles are the typical structure of association in dilute polymer solution. The block copolymer with longer B block length was found to be easier to form micelles; i.e., a lower critical micelle concentration (cmc) can be expected at a fixed temperature. Small molecular associates may also exist under certain conditions, usually in comparatively higher polymer concentrations. At concentrations much higher than the critical micelle concentration, the cross-linked micellar structure was predicted to exist by theoretical calculations or computer simulations,[3,11,12] based on the concept that for molecules of this type limited open molecular association accompanied closed association to micelles. However, direct observation by experiments was only reported in 2% $B_{12}E_{260}B_{12}$ solution for the $B_nE_mB_n$ triblock copolymer systems.[10] For similar triblock copolymers with shorter B blocks, no direct evidence has been revealed. Yang et al. concluded that there should be several equilibria in solution:[6] between single molecules and linked molecules (molecular associates), between molecules and micelles, as well as between micelles and linked micelles.

[†] Department of Chemistry, State University of New York at Stony Brook.
[‡] Department of Materials Science and Engineering, State University of New York at Stony Brook.
[§] Brookhaven National Laboratory.
[⊥] The Dow Chemical Co.
[||] Current address: 54-109, Chang-Chun-Yuen, Peking University, Beijing.
[▽] Current address: Chemistry Department, Tamkang University, Tamsui, 25137, Taiwan, Republic of China.
[⊗] Abstract published in *Advance ACS Abstracts,* October 1, 1997.

S1089-5647(96)03810-2 CCC: $14.00

In this article, a study by laser light scattering (LLS) and small-angle neutron scattering (SANS) on one of the triblock copolymers belonging to poly(oxybutylene)−poly(oxyethylene)−poly(oxybutylene), abbreviated as $B_6E_{46}B_6$ is reported. This block copolymer has six B units for each end block and happens to be at the intermediate position among the other similar block copolymers. This makes it valuable for comparison. The combination of LLS and SANS results can provide detailed information on the structure of polymer molecules and molecular associates. Former studies on this copolymer revealed that in 10 wt % polymer solution at 25 °C, molecular associates existed.[10] However, at lower temperatures and lower concentrations we did not find such structure. We present a study on the different existing forms of $B_6E_{46}B_6$ molecules, mainly focusing on the formation and the structure of micelles and of supramolecular associates in aqueous solution and compare those with other $B_nE_mB_n$ type triblock copolymers.

Experimental Section

Preparation and Characterization of Copolymers. Into a closed system, stirred steel reaction vessel was placed 339 g of 1,2-propylene glycol (The Dow Chemical Company) containing 0.66% (w/w) dissolved KOH (Aldrich Chemical Co.). The reactor was successively purged with nitrogen three times to rid adventitious oxygen. Temperature was increased to 130 °C and 1905 g of ethylene oxide (EO) (The Dow Chemical Company) was fed at a rate to maintain an internal pressure of below 70 pounds per square inch absolute (PSIA). Following addition of EO the reaction temperature was maintained at 130 °C until the pressure drop over a 1 h period was less than 0.5 PSIA. By phthalic anhydride analysis, the diol polymer was shown to contain 6.64% (w/w) hydroxyl groups (OH) corresponding to a number-average molecular weight of 512. The unneutralized liquid intermediate polymer was cooled to room temperature, removed from the reactor and stored under nitrogen.

Next 878 g of the intermediate poly(ethylene glycol) was added to the reactor along with 7.03 g of KOH. After a nitrogen purge sequence the temperature was taken to 100 °C for 30 min with stirring to affect dissolution of the KOH. The reactor temperature was increased to 130 °C and 2805 g of EO was delivered under the same pressure constraints mentioned above. After digest, a 132 g sample was taken and the molecular weight was determined to be 2024 (1.68% OH). In a subsequent feed, also at 130 °C, 1705 g of 1,2-butylene oxide was added to form the hydrophobic end blocks. The final molecular weight of the block copolymer was determined to be 2881 (1.18% OH). The reactor contents were cooled to 60 °C and 7.61 g of glacial acetic acid (Fisher Scientific Company) was added to neutralize the basic catalyst. Potassium acetate from the neutralization was not removed from the product. The kinetic viscosity of the product was 62.0 cSt at 212 °F.

Purification of the Sample. An aqueous solution of raw $B_6E_{46}B_6$ was quite nebulous. Hexane was used to extract impurities from the bulk copolymer at 35 °C. The hexane was then removed under vacuum at the same temperature. After one cycle, the polymer solution became clear. However, dynamic light scattering (DLS) still revealed the presence of very large particles with hydrodynamic radius of more than 100 nm, as shown in Figure 1, even at fairly low polymer concentrations (e.g., at 5.0 mg/mL). By using the same purification method four times, the large particle peak in the size distribution plot from DLS disappeared, and the scattering intensity of the solution went down appreciably.

Solution Preparation. Triblock copolymer solutions were prepared by diluting a stock solution (100 mg/mL). The stock solution was obtained by dissolving a known amount of purified copolymer in distilled water at 5 °C. To prepare dust-free solutions for light scattering measurements, the solutions were filtered through Millipore sterile membrane filters (0.1 μm pore size) into 17-mm-o.d. light scattering cells, which had been rinsed with distilled acetone to ensure a dust-free condition before use.

Laser Light Scattering (LLS). We used a standard, laboratory-built light scattering spectrometer (with 488 nm argon ion laser) capable of both absolute integrated scattered intensity and photon correlation measurements at different scattering angles. Static light scattering (SLS) experiments were performed at scattering angles between 30° and 140°. Photon correlation spectroscopy measurements were made by means of a Brookhaven 9000 AT digital correlator. Measurements were usually performed at scattering angles of 45°, 60°, 90°, and 120°.

The basis for data analysis of SLS is the Rayleigh−Gans−Debye equation, valid for small, interacting particles in the form[13]

$$Hc/R_{90} = 1/M_w + 2A_2c \tag{1}$$

where $H \equiv 4\pi^2 n_{Bz}^2 (dn/dc)^2/N_A\lambda^4$ is an optical parameter with n_{Bz} being the refractive index of benzene, N_A is Avogadro's constant, λ is the laser wavelength (488 nm), M_w is weight-average molecular weight; A_2 is the second virial coefficient, and dn/dc is the refractive index increment. For this copolymer, $dn/dc = 0.133 \pm 0.002$ cm^{3}g^{-1} at 30 °C.[14] R_{90} is the Rayleigh ratio of the polymer solution at 90°, and it equals $R_{Bz,90}(I - I_0)/I_{Bz}(n^2/n_{Bz}^2)$, where $R_{Bz,90}$ is the Rayleigh ratio of benzene at 90°, with the value of 2.91×10^{-5}/cm at 488 nm;[15] I, I_0, I_{Bz} are the scattered intensities of the solution, the solvent, and benzene, respectively; and n is the refractive index of the solvent. From static light scattering measurements, we can determine M_w and A_2.

Dynamic light scattering (DLS)[15] measures the intensity−intensity time correlation function $G^{(2)}(\Gamma)$ by means of a multichannel digital correlator.

$$G^{(2)}(\Gamma) = A(1 + b|g^{(1)}(\tau)|^2) \tag{2}$$

where A, b, and $|g^{(1)}(\tau)|$ are, respectively, the background, a coherence factor and the normalized electric field correlation function. The field correlation function was analyzed by the constrained regularized CONTIN[16] method, to yield information on the distribution of the characteristic line width (Γ) from

$$|g^{(1)}(\tau)| = \int G(\Gamma) e^{-\Gamma\tau}\, d\Gamma \tag{3}$$

The normalized distribution function of the characteristic line width $G(\Gamma)$ so obtained can be used to determine an average apparent diffusion coefficient

$$D_{app} = \Gamma/q^2 \tag{4}$$

where $q[(4\pi n/\lambda)\sin(\theta/2)]$ is the magnitude of the scattering wave vector. The apparent hydrodynamic radius $R_{h,app}$ is related to D_{app} via the Stocks−Einstein equation:

$$D_{app} = kT/\xi \tag{5}$$

with the Stokes relation

$$\xi = 6\pi\eta R_{h,app} \tag{6}$$

where k is the Boltzmann constant and η is the viscosity of

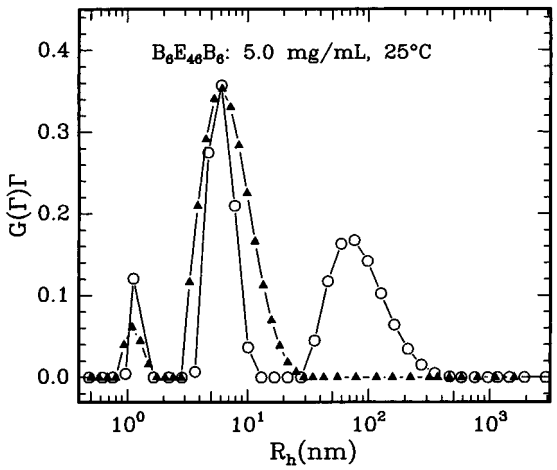

Figure 1. Typical size distribution of $B_6E_{46}B_6$ in aqueous solution after purification by hexane one time (open circles) and four times (filled triangles), measured by DLS with CONTIN analysis. The large aggregates due to impurities had a hydrodynamic radius ($<R_h>$) of about 100 nm.

water at temperature T. From DLS measurements, we can obtain the particle-size distribution in solution from a plot of $\Gamma G(\Gamma)$ versus $R_{h,app}$, with $\Gamma_i G(\Gamma_i)$ being proportional to the scattering intensity of particle i having an apparent hydrodynamic radius $R_{h,i}$. The subscript apparent is used to denote DLS measurements performed at finite concentrations when interparticle interactions have been neglected. The Stokes relation is valid for a large sphere moving through a homogeneous, continuous, incompressible fluid. In our case, we have assumed that the Stokes relation is valid for polymer colloids moving in a solvent. It is noted that deviations could become important when the solute particles are comparable in size to that of the solvent molecules.[17]

Small-Angle Neutron Scattering (SANS). SANS experiments were performed by using the biology small-angle neutron scattering spectrometer[18] located at H9B in the High-Flux Beam Reactor (HFBR) of Brookhaven National Laboratory. Cold neutrons were derived from a liquid-hydrogen cold-neutron source located in the beam thimble of the H9B beam line. The wavelength was set at 7.29 Å and had a spread in $\Delta\lambda/\lambda$ of less than 10%. Samples were prepared in D_2O and placed in capped quartz cells with a path lengths of 2 mm. A two-dimensional detector was used, and the scattered intensity profiles were derived by circular integration of the two-dimensional pattern. With the current setup, the smearing effects due to wavelength spread and beam divergence were negligible. The experiment temperatures were between 5.0 and 45.0 °C. The correction of measured scattered intensity profiles has been described elsewhere.[19]

Results and Discussion

The Impurities. After the $B_6E_{46}B_6$ triblock copolymer was purified by hexane only once, the aqueous polymer solution was clear, but DLS measurements showed the existence of some very large particles (>100 nm) (Figure 1, open circles). Such particles should have a very strong capability to scatter incident light. From Figure 1, the contribution to the total scattered intensity due to the large aggregates is less than that of micelles; this denotes that there is only a very small amount of such aggregates in solution. By using hexane to purify the polymer sample four times, the peak at 100 nm disappeared (Figure 1, filled triangles), and at the same time the total scattered intensity decreased greatly. The left two peaks are represented as unimers and micelles, respectively. From the above we can conclude that the large aggregates (or the impurities) are formed by some more hydrophobic components, e.g., some block copolymers with longer B blocks or shorter E blocks. The other two peaks did not show any change in position before and after removing the impurities, so we can be sure that the majority of the block copolymers (which have the formula $B_6E_{46}B_6$, and maybe a little extra fraction which were even more hydrophilic than $B_6E_{46}B_6$) were still in solution. In the latter case, the broader micellar peak can be attributed to the poor signal/noise ratio, which became a problem because the total scattered intensity was much lower.

Clouding Temperature and Phase Diagram. The clouding temperature, defined as the temperature at which phase separation occurs, is often determined by visual observation or by monitoring the variation of the incident laser beam intensity transmitted through the solution. We used SLS to measure the clouding point of the solution. The onset of this phase transition results in strong scattered intensity in SLS when the solution first becomes cloudy in appearance. The clouding temperature can be measured by a sharp change in the scattered intensity with increasing temperature. For dilute $B_6E_{46}B_6$ polymer solutions (0.1%−5%), the clouding temperatures were between 34 and 38 °C.

By combining the data for the concentration dependence of the clouding temperature, the temperature dependence of the cmc, and the critical micelle temperature (cmt) result (details following), the phase diagram of $B_6E_{46}B_6$ copolymer in dilute aqueous solution can be constructed; it has been published elsewhere.[20] There are three areas in the temperature versus concentration diagram: the unimer region, the region where unimers and micelles coexist, and the two-phase region.

Unimer Region. At low copolymer concentrations (e.g., 1% at 5 °C), the $B_6E_{46}B_6$ copolymers exist as single polymer chains. SLS measurements were used to determine the weight-average molecular weight of the copolymer by using eq 1. Figure 2a shows the result with $M_w = 2.95 \times 10^3$ g/mol which is in good agreement with the nominal molecular weight of 2890 g/mol, obtained from the chemical formula of $B_6E_{46}B_6$. The negative second virial coefficient ($A_2 = -2.5 \times 10^{-3}$ mol cm^3/g^2 at 5 °C) suggests that the solute−solute interactions are quite strong. It is interesting to make a comparison with another similar block copolymer, $B_5E_{91}B_5$, whose unimers had an A_2 of -6.9×10^{-4} mol cm^2/g^2 at 25 °C.[8] Usually at higher temperatures the polyalkylene blocks will become more hydrophobic, and therefore a more negative A_2 value can be expected. Now $B_5E_{91}B_5$ has a less negative A_2 even at higher temperatures; one explanation is that the longer hydrophobic B blocks and shorter hydrophilic E blocks lower the solubility of $B_6E_{46}B_6$ unimers in water and the interactions among solute molecules become much stronger.

In DLS measurements at 10 mg/mL and 5 °C, only one peak was observed with an average hydrodynamic radius ($<R_h>$) of about 1.2 nm, as shown in Figure 2b. Here the Y axis is represented as $G(\Gamma)\Gamma$, with $G(\Gamma)$ being the normalized characteristic line width distribution function. The small particle size and the molecular weight determination from SLS confirmed the presence of mainly unimers.

From the angular dependence of the scattered intensity, the average particle radius of gyration ($<R_g>$) can be determined by SLS if the particles have sizes in the range between 20 and 200 nm. However, unimers and even micelles of $B_6E_{46}B_6$ triblock copolymers were too small to be measured by SLS. SANS was then used to measure the particle sizes. Figure 3 shows the scattering curves of SANS in a Guinier plot with the $B_6E_{46}B_6$ triblock copolymers being dissolved in D_2O. There is

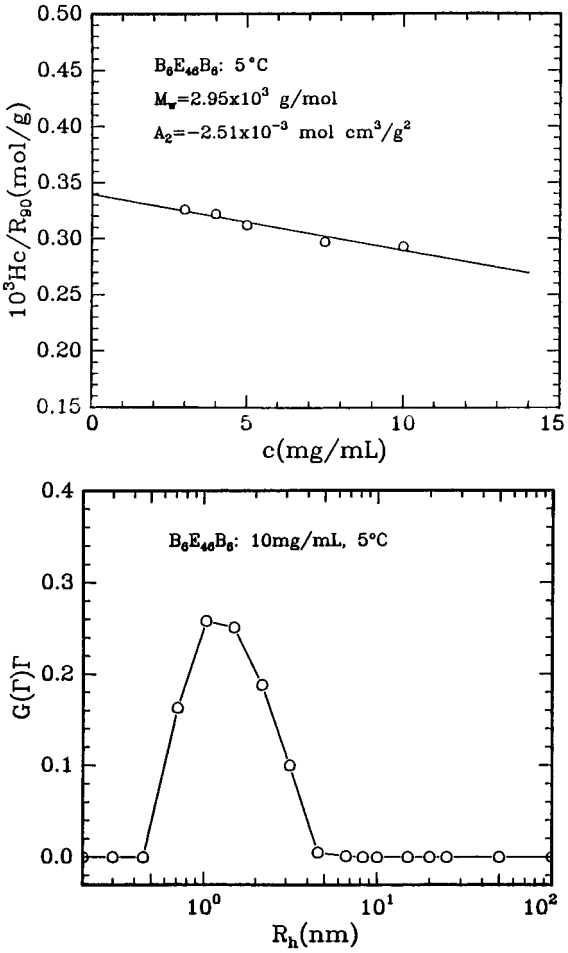

Figure 2. (a) Determination of the weight-average molecular weight and the second virial coefficient of $B_6E_{46}B_6$ single molecules by SLS. (b) DLS with CONTIN analysis showing $B_6E_{46}B_6$ unimer at the hydrodynamic radius (R_h) of about 1.2 nm.

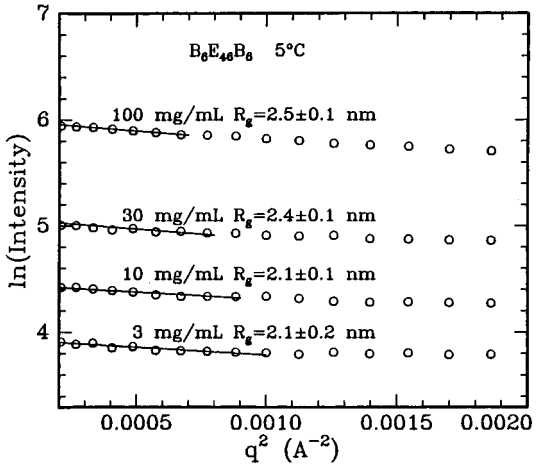

Figure 3. Determination of R_g of $B_6E_{46}B_6$ unimers and micelles by SANS.

a small difference in the scattering contrast between the two kind of blocks. However, when compared with the scattering contrast between the deuterated solvent (D_2O) and the hydrogenated solute, this difference can be neglected. The lowest two curves in Figure 3 are from solutions of 3 and 10 mg/mL, and from LLS we knew that they were mainly unimer solutions at 5 °C. Therefore we can determine the unimer $<R_g>$ value of about 2.1 nm. The ratio of $<R_g>/<R_h>$ is a characteristic parameter describing the polymer architecture, chain conformation, and polydispersity. It is known that $<R_g>/<R_h>$ is 0.773, ~1.8, and ~2 for a uniform sphere, a polydisperse linear coil, and a rodlike linear chain, respectively.[21−23] In this polymer solution, the comparatively large value of $<R_g>/<R_h>$ (1.8) suggested that the single polymer molecules in solution might exist as flexible linear coils.

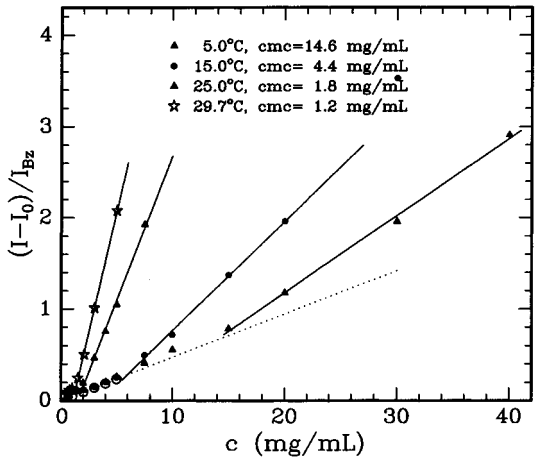

Figure 4. Determination of critical micelle concentrations (cmc) and their temperature dependence of $B_6E_{46}B_6$ aqueous solution by SLS.

TABLE 1: Micellar Parameters Derived from Static Light Scattering

T (°C)	cmc (mg/mL)	M_{mic} (g/mol)	n_w	A_2 (mol cm^3/g^2)
5.0	14.6	5.15×10^3	2	1.8×10^{-4}
15.0	4.4	7.19×10^3	2.5	2.0×10^{-5}
25.0	1.8	2.05×10^4	7	-3.0×10^{-5}
29.7	1.2	3.52×10^4	12	-1.0×10^{-4}

Similar studies on $B_5E_{91}B_5$ showed that its unimers have a R_g of about 2.5 nm and R_h of about 2.1 nm. That is, for $B_5E_{91}B_5$, the ratio of R_g over R_h becomes lower than that of $B_6E_{46}B_6$, indicating a less compact structure for $B_5E_{91}B_5$ unimers in water.

Critical Micelle Concentration (cmc), Critical Micelle Temperature (cmt), and Association Number (n_w). When the concentration of $B_6E_{46}B_6$ copolymer solution or the solution temperature was increased, the scattered intensity increased greatly, indicating that some larger structures, e.g., micelles, had formed. The critical micelle concentration can be defined as the concentration at which the static light scattering intensity departs significantly from a baseline value established for single triblock copolymer molecules. Figure 4 shows a plot of $(I - I_0)/I_{Bz}$ versus polymer concentration at different temperatures, where I, I_0, and I_{Bz} are the scattered intensity of polymer solution, distilled water, and benzene, respectively. The departure point of the scattered intensity curves from the baseline can be clearly determined in Figure 4. The cmc's extrapolated by linear regression of these intensity ratios are given in Table 1. Similar to other $B_nE_mB_n$ type block copolymers in water, at higher temperatures the cmc of $B_6E_{46}B_6$ became smaller, from 14.6 mg/mL at 5 °C to 1.19 mg/mL at 29.7 °C. Notice that at 30 °C, $B_5E_{91}B_5$ has a cmc about 7.4 mg/mL.[9] The effect of chain architecture on micellization is quite obvious.

When applied to micellar solutions to calculate the micellar association number, the Debye equation has the form

$$H(c - c_{cmc})/[R_{Bz}(I - I_{cmc})n^2/(I_{Bz}n_{Bz}^2)] = 1/M_w + 2A_2(c - c_{cmc}) \quad (7)$$

where I_{cmc} represents the scattered intensity at cmc. Equation 7 can be utilized under the assumptions that the association number is a constant at a fixed temperature and that the concentration of unimers does not increase above its value at

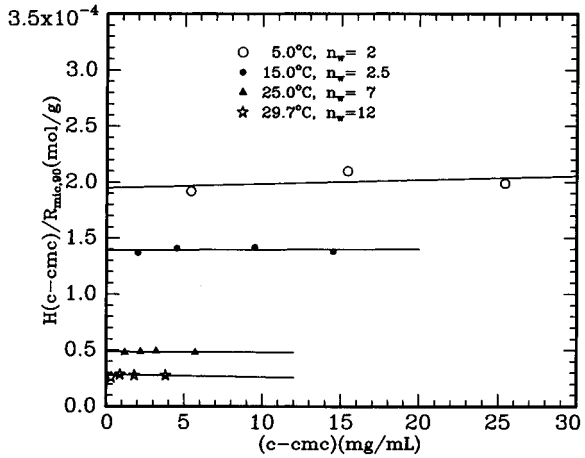

Figure 5. Determination of association numbers of $B_6E_{46}B_6$ micelles by SLS. The association number increases with increasing temperature.

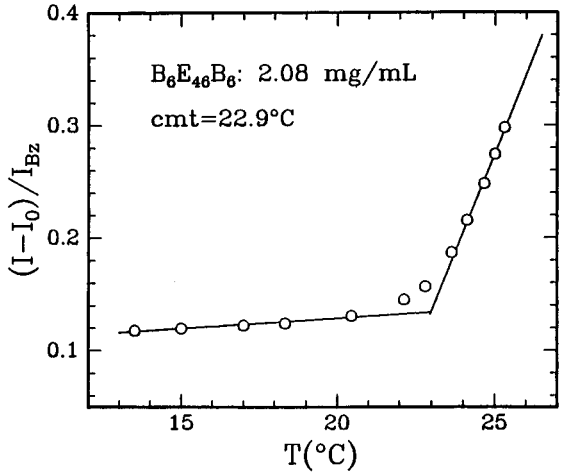

Figure 6. Critical micelle temperature (cmt) measurements by SLS.

the cmc. Both of these premises are met when the polymer concentrations are only several times larger than the cmc. From this equation we can determine the micellar weight-average molecular weight, the corresponding association number of micelle near the cmc, and A_2 for micelle particles at different temperatures, as shown in Figure 5. The weight-average association number (n_w) and the A_2 of the micelles became higher at higher temperatures, as listed in Table 1. The A_2 values have about a 10% error. The small A_2 values indicate that micelle solutions are quite like ideal solutions. In the unimer region we had a negative A_2 value. The A_2 change could be attributed to the fact that the hydrophobic B blocks entered the cores of micelles, resulting in a lowering of the solute−solute interactions. The same phenomenon has also been observed in $B_5E_{91}B_5$ solutions, where the A_2 of micelles had a positive value (about 10^{-5} mol cm^3/g^2) at 25 °C and became negative at higher temperatures (about -10^{-4} mol cm^3/g^2 at 45 °C).

The critical micelle temperature (cmt) can be measured by SLS, similar to the clouding point measurements. As an example, Figure 6 shows that the cmt = 22.9 °C at c = 2.08 mg/mL.

In the micellization process, the expressions for free energy, enthalpy and the change of entropy are as follows:[9]

$$\Delta G^\circ = RT \ln(\text{cmc}) \tag{8}$$

$$\Delta H^\circ = R[\text{d} \ln(\text{cmc})/\text{d}(1/T)] \tag{9}$$

or

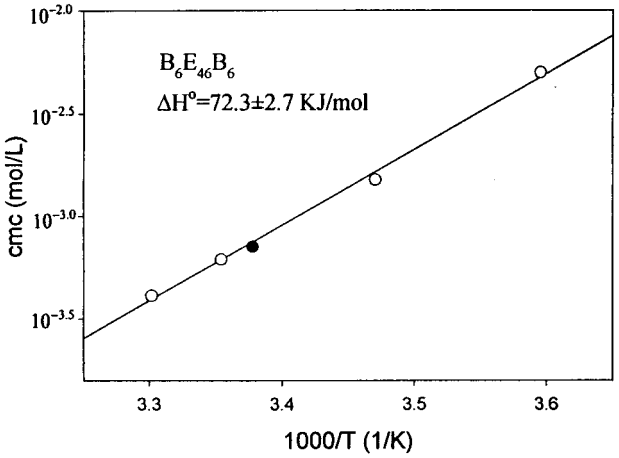

Figure 7. Thermodynamics of micellization. Open circles are from cmc data, and the filled circle is from cmt data.

TABLE 2: Clouding Temperature at 10 mg/mL and cmc at 20 °C of $B_nE_mB_n$ Triblock Copolymers

	clouding temperature (°C)	cmc (mg/mL)
$B_4E_{40}B_4$	61	190[7]
$B_5E_{39}B_5$	43	20[7]
$B_5E_{91}B_5$	52	20.6[9]
$B_6E_{46}B_6$	35	3.2
$B_7E_{40}B_7$	26	1.0[7]
$B_{12}E_{260}B_{12}$	25	0.04[24]
$B_{12}E_{76}B_{12}$	12	

$$\ln(\text{cmc}) = \Delta H^\circ / RT + \text{constant} \tag{10}$$

and

$$\Delta S^\circ = (\Delta H^\circ - \Delta G^\circ)/T \tag{11}$$

Figure 7 shows a plot of ln(cmc) versus 1/T for the $B_6E_{46}B_6$ copolymer. From its slope we got $\Delta H^\circ = 72 \pm 3$ kJ/mol. At 25 °C, $\Delta G^\circ = -18$ kJ/mol and $\Delta S^\circ = 304$ J/(mol·K). Equation 8 assumes a large value for n_w. However, Figure 7 shows a very good linear relationship in a plot of ln(cmc) versus 1/T. Therefore, we have ignored the requirement for large n_w and assume that eq 8 is applicable in our case. The length of the B end blocks has been shown to be crucial for the ΔH° value of the copolymer: the longer the B blocks, the smaller the ΔH° value. For example, $B_5E_{91}B_5$ has a ΔH° of about 80 kJ/mol,[9] but for $B_{12}E_{260}B_{12}$, ΔH° is only about 24 kJ/mol.[10] The positive ΔS° value indicates that the micellization is an entropy-driven process.

The clouding temperatures and the cmc values for several $B_nE_mB_n$ triblock copolymers[7,24] are listed in Table 2. This comparison shows that, with increasing length of the B block, both the clouding temperature and the cmc values decrease. However, the clouding point is also related to the length of hydrophilic E blocks; e.g., the $B_5E_{91}B_5$ copolymer has a clouding temperature 8 °C above that of $B_5E_{39}B_5$ at the same concentration. A systematic and quantitative study of the phase behavior of $B_nE_mB_n$ type block copolymers is in preparation. However, the cmc is determined mainly by the B block length, while the E block length has little effect; e.g., $B_5E_{39}B_5$ and $B_5E_{91}B_5$ have very similar cmc values. Under similar conditions, e.g., 5 °C down from the clouding point, the $B_nE_mB_n$ type block copolymer micelles have small association numbers (i.e., 10−20 for the above condition). Also, there is evidence that the association number depends on the length of B blocks while the hydrodynamic radius of the micelles depends on the length of E blocks. A detailed description will be presented in another article.

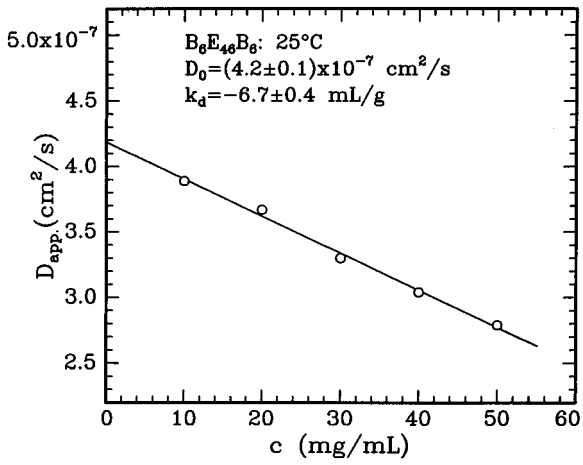

Figure 8. Concentration dependence of apparent diffusion coefficients of $B_6E_{46}B_6$ micelles.

Dynamic Light Scattering in the Micellar Region. Above certain temperatures (≥15 °C), two modes were observed in dynamic light scattering from triblock copolymer solutions in the micellar region, as shown in Figure 1 (filled triangles). A weak mode had an $<R_h>$ of about 1.2 nm, which could be identified with the unimers having a similar size as shown in Figure 2b. Another mode had an $<R_h>$ of 6−9 nm, which was identified with the micelle particles. This illustrates that the micelles are in equilibrium with single polymer molecules together with the narrow size distribution of micelles. We can consider the supramolecular formation to be a closed association process:

$$n\mathrm{A} \leftrightarrow (A)_n \tag{12}$$

The DLS at very low temperatures often gave broad peaks from the CONTIN analysis, partly due to the poor signal-to-noise ratio from the low scattered intensity. However, the nature of the association process may also change, as will be discussed in later paragraphs.

Figure 8 shows that at 25 °C, the apparent diffusion coefficient (D_{app}) of the micelle increases with increasing concentration. The unimers have an average D_{app} value of about 2.5×10^{-6} cm^2/s, and show little concentration dependence. From the characteristic line width distributions, the apparent diffusion coefficients (D_{app}) can be calculated. Then D_0 can be obtained by extrapolating D_{app} to zero concentration:[9]

$$D_{app} = D_0(1 + k_d c) \tag{13}$$

This expression has been truncated after the second term and it is correct in the dilute solution regime. The parameter k_d is related to the thermodynamic second virial coefficient, A_2, through the equation

$$k_d = 2A_2M_w - k_f - 2\nu \tag{14}$$

where k_f is the frictional coefficient and ν is the partial specific molar volume of the micelle. If the quantities M_w, k_f, and ν are independent of concentration, the sign of k_d depends on the sign and magnitude of A_2, which in turn depends on the nature of intermicellar interactions.[7] For $B_6E_{46}B_6$, the negative slope in Figure 8 implies a substantial attractive contribution to their intermicellar interactions. Recall that at 25 °C the A_2 of the micelle solutions near cmc has a small negative value. At current polymer concentrations, if we were to use the hard sphere model to describe the micelles, which had a k_f value of about 6.0 and the measured $k_d = -6.7 \pm 0.4$ mL/g, the value of ν would be small and could be neglected. The calculation would lead to a negative A_2 with a larger magnitude (around 3×10^{-5} mol cm^3/g^2) when compared with A_2 values at low polymer concentrations. This finding is consistent with the view of micelles having a fraction of their B blocks extended into the solvent and thus becoming available for interactions, either with B blocks from chains originating from a second micelle or by entering the core of a second micelle.

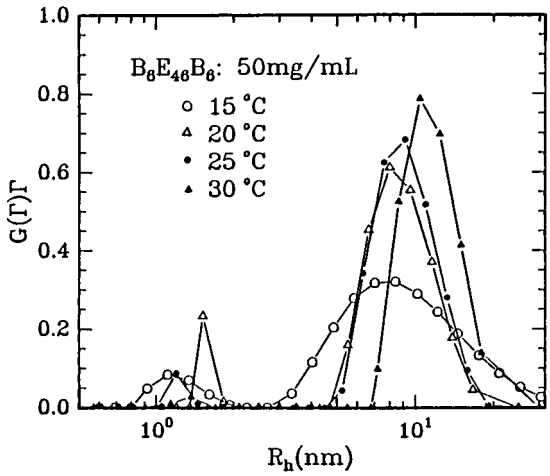

Figure 9. Temperature dependence of R_h of $B_6E_{46}B_6$ micelles. Data are from Table 3b.

TABLE 3: Concentration and Temperature Dependence of $<R_h>$

(a) Concentration Dependence of R_h at 25 °C

concn (mg/mL)	$<R_{h,mic}>$ (nm)	$<R_{h,uni}>$ (nm)	I_{mic}/I_{uni}
10	6.3	0.9	25
20	6.6	1.0	27
30	7.5	1.5	29
40	8.1	1.4	31
50	8.8	1.3	35

(b) Temperature Dependence of R_h at 50 mg/ML

T (°C)	$<R_{h,mic}>$ (nm)	$<R_{h,uni}>$ (nm)	I_{mic}/I_{uni}
15	8.0	1.2	10
20	8.5	1.5	14
25	8.8	1.3	35
30	11.0	1.3	81

Figure 9 shows that, for $B_6E_{46}B_6$ at $c = 50$ mg/mL, the average value of $<R_h>$ increases with increasing temperature. At the same time, the micellar size distribution becomes narrower. From Table 3 we can find that the intensity ratio of micelles to unimers becomes higher with increasing temperature or concentration, meaning that the association equilibrium (eq 12) has shifted, favoring micelle formation. The increase of the ratio of the micellar peak over the unimers' peak with increasing concentration at certain temperature seems quite slow, showing that the micellar association number roughly maintains a constant value under isothermal conditions. However, at a certain concentration, the value of I_{mic}/I_{uni} increases greatly with increasing temperature, suggesting that the association number of micelles experiences a great increase. This is consistent with the results from SLS, reported above in Table 1.

SANS Study of Micelle Solutions. Considering the small size of the $B_6E_{46}B_6$ unimers, we resorted to SANS to measure their size in D_2O solutions. Representative Guinier plots and radii of gyration are shown in Figure 3. Similar measurements were also performed at 15, 25, and 30 °C. Unfortunately, in many cases the micelles coexist with unimers in solution. Thus, the SANS only give us an average $<R_g>$ of all the particles. At concentrations only a little higher than the cmc, we can

TABLE 4: Aggregation Numbers and Micellar Sizes at Different Temperatures

T(°C)	n_w	$<R_{h,mic}>$ (nm)	$<R_{g,mic}>$ (nm)	$<R_{g,mic}>^3/n_w$ (nm^3)	$<R_{g,mic}>/<R_{h,mic}>$
	1	1.2		9.3	1.8
5.0	2		2.5	7.8	
15.0	2.5	6.3	2.7	7.8	0.43
25.0	7	6.5	3.6	6.7	0.55
30.0	12	5.7	3.9	4.9	0.68
					0.77 (hard sphere)

consider that the concentration of the unimers is essentially that of the cmc. We assume that the association number of micelles has remained constant. As mentioned before, the unimers' $<R_g>$ is 2.1 nm. A larger value of $<R_g>$ indicates the existence of micelles in solution. By checking the cmc values at different temperatures, we can see that each cmc value obtained from SLS is between the two adjacent measured concentrations from SANS which represent the unimer region and the micelle region; i.e., the SANS results are consistent with SLS results. At higher temperatures (≥25.0 °C), micelles have formed even in the lowest measured concentration. We can calculate the $<R_{g,mic}>$ of the micelles alone from the experimentally determined $<R_{g,ave}>$ and that of the unimers $<R_{g,uni}>$ obtained at low concentrations and temperatures by using the following formula:

$$C_{uni}M_{uni}<R_{g,uni}>^2 + C_{mic}M_{mic}<R_{g,mic}>^2 = C_{ave}M_{ave}<R_{g,ave}>^2 \quad (16)$$

where C, M, and $<R_g>^2$ are the concentration, molecular weight, and the radius of gyrations of unimers, micelles, and mixtures, respectively. The calculated results are listed in Table 4. In Table 4, n_w is the aggregation number and $<R_{h,mic}>$ is the hydrodynamic radius of the micelles (from DLS). For $<R_{h,mic}>$, at different temperatures, we picked up different polymer concentrations which were above but not far away from cmc. From Table 3, it is obvious that the $<R_g>$ of micelles increases with the aggregation number. All the calculations we did were based on the premise that $<R_{g,uni}> = 2.1$ nm. In fact, at higher temperatures, the B blocks may become more hydrophobic and the shape of the unimers might change so that $<R_{g,uni}>$ could become smaller. However, this change had very little effect on the value of $<R_{g,mic}>$. For example, at 30 °C, even if the $<R_{g,uni}>$ value were to decrease 50% to 1.1 nm, the calculated $<R_{g,mic}>$ would increase by only about 2%, which is within the experimental error. The ratio of $<R_{g,mic}>^3$ to the association number n_w can be regarded as an index for the structure of the micelles. It should be a constant for similar structures. However, as shown in Table 4, the $<R_{g,mic}>^3/n_w$ decreases with increasing temperature. It is easy to understand that the B blocks become more hydrophobic at higher temperatures, so part of the B blocks, which are dangling in the solution, at high temperatures will go back to the core of the micelles. The E blocks also become more hydrophobic at high temperatures, so that the corona of the micelles also become more compact. Similar conclusions can also be drawn from the ratio of $<R_{g,mic}>$ to $<R_{h,mic}>$. For a solid sphere, the ratio is equal to 0.77. For $B_6E_{46}B_6$ micelles, the calculated ratios (Table 3) are between 0.43 and 0.68, suggesting that more mass of the micelles should distribute near the micellar center, in reasonable agreement with the prediction of a core−shell model. With increasing temperature, this ratio becomes larger and approaches that of the solid sphere, indicating that the micelles shrink to become more compact. However, at low temperatures, the $<R_{h,mic}>$ values appear to be too large; i.e., for a 20 mg/mL copolymer solution at 15 °C, $n_m = 2.5$ and $<R_{h,mic}> = 6.3$ nm. The polymer density in one micelle, calculated from micellar mass and the hydrodynamic volume is 12 mg/mL, which is even lower than the average polymer density in solution! The same phenomenon was also observed in $B_5E_{91}B_5$ aqueous solution.[9] With the association number being quite small (2.5), it is difficult to see that the association structure can be perfect core−shell micelles. The extraordinarily large $<R_h>$ may imply that the association is an open structure, with B blocks forming small clusters to connect single polymers molecules. The DLS results of these clusters yielded very broad distributions, supporting the presence of an open structure. However, the CONTIN results may be affected by the poor signal-to-noise ratio, which can also result in apparent broad peaks, making a more definitive conclusion difficult at this time.

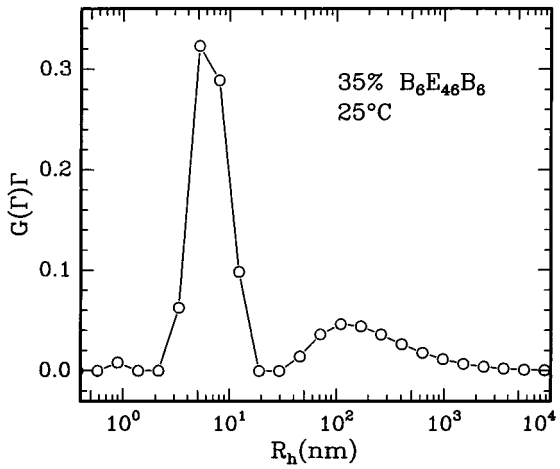

Figure 10. CONTIN analysis of 35% $B_6E_{46}B_6$ solution. A third peak which represents supramicellar structures ($R_h \approx 100$ nm) is observed.

Higher Order Structures at Higher Polymer Concentrations. Unimers and micelles tend to coexist at high polymer concentrations, even though the aggregation number may increase gradually. At very high concentrations (e.g., 35% in mass) and at room temperature, another extra-slow mode can be observed by DLS, with an apparent hydrodynamic radius of more than 100 nm (Figure 10). This mode can be understood as the supramicellar structure formed by the cross-linking of micelles, e.g., some of the two end B blocks of the triblock copolymers are now located in two neighboring micelles. At high polymer concentrations, the micelle−micelle distance becomes smaller, such that intermicellar structures become easier to form. However, the peak area ratio of micelles to supramicellar structures is quite high, indicating that micelles remain the majority species in the polymer solution. The broad distribution of the size of the supramolecular structures reveals that the intermicellar cross-linking is likely random association, with no firm association numbers or ordered structures.

Yang et al.[7] cited that some of the theoretical calculations and computer simulations have shown the intermicellar bridge structure can exist in $B_mE_nB_m$ triblock copolymer systems because of the nature of this kind of polymer molecules: their association behavior in water should be limited open molecular association accompanied by closed association to micelles. They obtained some indirect evidence from DLS experiments on such copolymers with $m = 4$, 5, or 7. However, no direct experimental evidence has been reported for copolymers with short B blocks. The only report on this structure was done by Zhou et al.[10,24] for the $B_{12}E_{260}B_{12}$ system by DLS. The long hydrophobic B blocks promote the polymer chains to form very strong intermicellar structures even in a 10% polymer solution.

Under the same condition, SANS gave a flat intensity profile without any peaks, suggesting that there were no globular

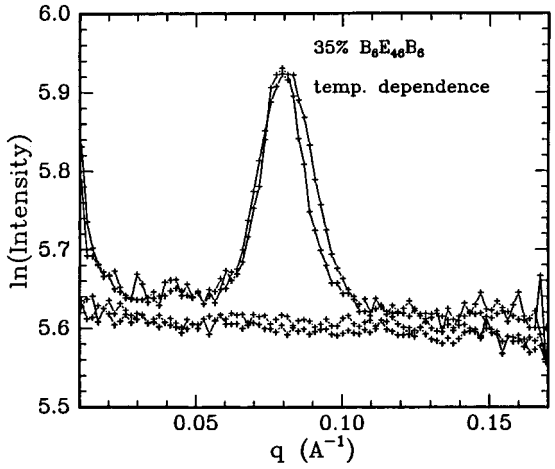

Figure 11. SANS profiles of 35% $B_6E_{46}B_6$ solution at different temperatures. The two curves which show a peak were measured at 5 and 15 °C, while the other two were obtained at 25 and 30 °C, respectively. The presence of a peak suggests microphase separation with a correlation length of about 8 nm.

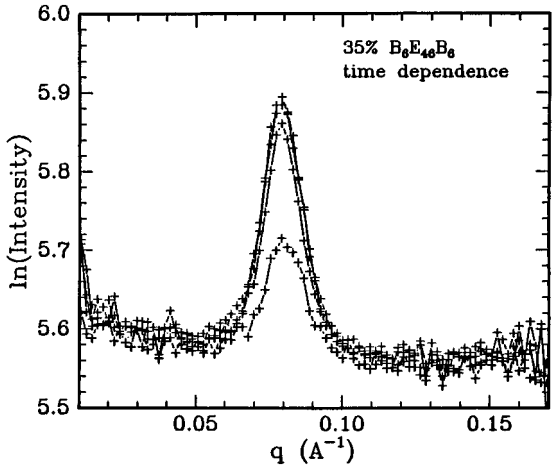

Figure 12. SANS profiles of 35% $B_6E_{46}B_6$ solution at 15 °C measured at 2-h intervals. The peak height increased with time.

structures in solution. However, when the sample was cooled to ≤15 °C, a peak was observed at $q = 0.078$/Å, which represented the presence of microphase separation. The micelle−micelle distance is about 8 nm, as shown in Figure 11. The extended E_{46} block has the length of about 16−17 nm, so 8 nm is reasonable as a bridging distance. At this temperature the sample became very viscous. The kinetics of microphase separation has been monitored by four consecutive SANS measurements, at 2-h intervals. Figure 12 shows that this process was quite slow as we can observe the growth of the peak with time.

Conclusions

1. Block copolymers are often less well-defined in composition homogeneity, causing complex states of aggregation in solution under appropriate temperature and concentration conditions. Organic solvent (hexane) was used to remove these hydrophobic impurities.

2. As evidenced by a combination of static and dynamic light scattering experiments for the triblock copolymer solution studied, three regions appear in sequence with increasing temperature. They are the unimer, the micelle, and the large aggregate regions.

3. Unimers of the triblock copolymer exist as linear coils; no unimolecular micelles have formed.

4. The formation of micelles obeys the closed-association process and is entropy-driven at higher temperatures (>15 °C). At lower temperature, some evidence seems to show that small molecular associates are possibly formed with an open structure. The cmc of $B_6E_{46}B_6$ triblock copolymers decreases with increasing temperature, while the aggregation number increases but its values are quite small. On the basis of the interaction among the micelles, the experiments seem to show the existence of some dangling B blocks in the solution.

5. At high concentrations, supramolecular structures which are due to the strong interactions among the micelles appear. When the temperature goes down, a slow phase-separation process can occur.

Acknowledgment. We gratefully acknowledge support of this work by the National Human Genome Research Institute (1R01HG0138601), the Department of Energy (DEFG0286ER-45237.013), and the Center for Biotechnology.

References and Notes

(1) Chu, B. *Langmuir* **1995**, *11*, 414, and references cited therein.
(2) Semenov, A. N.; Nyrkova, I. A.; Khokhlov, A. R. *Macromolecules* **1995**, *28*, 7491.
(3) Balsara, N. P.; Tirrell, M.; Lodge, T. P. *Macromolecules* **1991**, *24*, 1975.
(4) ten Brinke, G.; Hadziioannou, G. *Macromolecules* **1987**, *20*, 486.
(5) Raspaud, E.; Lairez, D.; Adam, M.; Carton, J.-P. *Macromolecules* **1994**, *27*, 2956.
(6) Yang, Z.; Pickard, S.; Deng, N.-J.; Barlow, R. J.; Attwood, D.; Booth, C. *Macromolecules* **1994**, *27*, 2371.
(7) Yang, Y.-W.; Yang, Z.; Zhou, Z.; Attwood, D.; Booth, C. *Macromolecules* **1996**, *29*, 670.
(8) Zhou, Z.; Chu, B. *Macromolecules* **1994**, *27*, 2025.
(9) Zhou, Z.; Chu, B.; Nace, V. M. *Langmuir* **1996**, *12*, 5016.
(10) Zhou, Z.; Chu, B.; Nace, V. M.; Yang, Y.-W.; Booth, C. *Macromolecules* **1996**, *29*, 3663.
(11) Nguyen-Misra, M.; Mattice, W. L. *Macromolecules* **1995**, *28*, 1444.
(12) Rodrigues, K.; Mattice, W. L. *Polym. Bull.* **1991**, 25, 239.
(13) Hiemenz, P. Z. *Principle of Colloid and Surface Chemistry*; Marcel Dekker Inc.: New York, 1985.
(14) Bedells, A. D.; Arafeh, R. M.; Yang, Z.; Attwood, D.; Padget, J. C.; Price, C.; Booth, C. *J. Chem. Soc., Faraday Trans.* **1993**, 89, 1235.
(15) Chu, B. *Laser light scattering;* Academic Press: Inc.: New York, **1990**.
(16) Provencher, S. W. *Biophys. J.* **1976**, 16, 29; *J. Chem. Phys.* **1976**, *64* (7), 2772.
(17) Kivelson, D.; Jensen, S. J.; Ahn, M.-K., *J. Chem. Phys.* **1973**, *58* (2), 428.
(18) Schneider, D. K.; Schoenborn, B. P. *In Neutrons in Biology;* Schoenborn, B. P., Ed.; Plenum: New York, 1984; pp 1766.
(19) Wu, G.; Chu, B.; Schneider, D. *J. Phys. Chem.* **1994**, *98*, 12018.
(20) Chu, B.; Liu, T.; Wu, C.; Zhou, Z.; Nace, V. M. *Macromol. Symp.* **1997**, *118*, 221.
(21) Huber, K.; Bantle, S.; Lutz, P.; Burchard, W. *Macromolecules* **1985**, *18*, 1461.
(22) Akcasu, A. Z.; Han, C. C. *Macromolecules* **1979**, *12*, 276.
(23) Nordmeier, E.; Lechner, D. *Polym. J.* **1989**, *21* (8), 623.
(24) Zhou, Z.; Yang, Y.-W.; Booth, C.; Chu, B. *Macromolecules* **1996**, *29*, 8357.